A STOCHASTIC SOURCE MODEL FOR SYNTHETIC STRONG-MOTION SEISMOGRAMS

William B. Joyner[I]
David M. Boore[I]

SUMMARY

Random processes are commonly used to generate synthetic accelerograms but generally without reference to a physical model. We propose here a stochastic source model whose parameters have physical meaning. The approach is illustrated by calculation of synthetic accelerograms for the 1966 Parkfield, California earthquake at the Temblor recording site.

INTRODUCTION

We present here a method for generating synthetic strong-motion seismograms for use as input in the dynamic analysis of structures or for the determination of response spectra or other ground-motion parameters. An important basis of the method is the concept that random variability is characteristic of earthquake source processes and must be incorporated into the source model for a realistic representation of the high-frequency end of the ground-motion spectrum.

Housner (1955) was an early proponent of stochastic models of the earthquake source. Haskell (1966) and Aki (1967) used the concept in analyzing earthquake spectra, and Hanks (1979) has consistently emphasized the role of random heterogeneities in source processes. Stochastic methods are widely used for simulating earthquake ground motion for engineering purposes, though generally without any reference to a specific source model (Bycroft, 1960; Housner and Jennings, 1964). Simulation of ground motion that has a time-varying spectrum is possible using recursive filters (Jurkevics and Ulrych, 1978). The work of Rascón and Cornell (1969) is noteworthy in that they described a method whereby synthetic accelerograms were derived from an explicit stochastic source model. Although our work is in the spirit of Rascón and Cornell, we have attempted to tie the parameters of our models more closely to the physical processes at the source. Our emphasis is on the high-frequency end of the spectrum and on sites close to the source. Butler, Kanamori and Geller (1975) have used a similar approach for computing long-period motions.

DESCRIPTION OF THE MODEL

There are three obvious ways in which the source could show random variability: (1) the velocity of rupture propagation could vary; (2) the total dislocation could vary from point to point on the fault; and (3) the shape of the dislocation-time function could vary from point to point on the fault. In the model we present here, only the total amplitude of the dislocation varies; the rupture velocity and the shape of the dislocation-time function are constant. We are also working on other models in which all three factors vary.

[I]U.S. Geological Survey, Menlo Park, California, USA 94025

The model is illustrated in Figure 1. The rupture front sweeps across the fault surface at constant velocity V_R. To simplify the computations we collapse the fault into a line, so we are dealing with a point source moving along a line. A very broad class of dislocation-time functions may be used; for the example to be shown here an exponential ramp is used, as illustrated in Figure 2.

The amplitude of the dislocation-time function is composed of a mean value plus a variation about the mean. We control the spectrum of the synthetic seismogram by specifying the autocorrelation function of the variable part of the dislocation amplitude; that is our stochastic description of the source. The spectra of real accelerograms tend to be more or less flat below the frequencies where attenuation controls the slope. Such a spectrum can be achieved very simply by choosing an autocorrelation function that is a negative exponential. This function is specified by a single parameter, the coherence length, which is the distance at which the autocorrelation function is down by a factor of 1/e. In the computation of the variable part of the dislocation amplitude, Gaussian white noise is generated by the computer, using a pseudo random number generator, and then is filtered with the aid of the Fast Fourier Transform by a filter designed to produce an output with the desired autocorrelation function. Starting with different samples of white noise we produce different synthetic seismograms, which form an ensemble representing the ground motion to be expected at the site.

Four parameters of the model are to be determined by fitting real strong-motion records, the mean dislocation amplitude $\overline{D}$, the standard deviation of the dislocation amplitude σ_D, the coherence length ℓ_c, and the rise time τ (Fig. 2). To reduce the number of degrees of freedom we impose two conditions.

$$\overline{D} = \sigma_D \qquad \text{Eq. 1}$$

$$\ell_c / V_R = \tau \qquad \text{Eq. 2}$$

The first condition is not so arbitrary as might seem at first glance. If $\overline{D}$ greatly exceeds σ_D, the model ceases to be stochastic in a meaningful sense, and, if σ_D greatly exceeds $\overline{D}$, reversal of motion is implied over a significant portion of the length of the fault, given the Gaussian distribution of D. This leaves two free parameters σ_D and τ. Our strategy for subsequent work will be to evaluate these parameters for past earthquakes by fitting strong-motion records and use the results as a basis for selecting values for the parameters in the case of design earthquakes.

The source is placed in a homogeneous halfspace with modifications to the solution to allow for the effects of low-velocity material near the surface at the recording site and in the fault zone. Without the allowance for low velocity near the surface, the synthetic seismograms would not have realistic amplitude ratios between the horizontal and vertical components. There is substantial evidence for low P velocities in the San Andreas fault zone (Mayer-Rosa, 1973; Healy and Peake, 1975; Marks and Bufe, 1979); presumably S velocities in the fault zone are also low. In the example to be shown the recording site is at a node for SV waves, but the S amplitudes

on the radial component are nearly as large as those on the transverse component. The simplest explanation of the observed amplitude ratio is that the rays are refracted in going from the fault zone into the higher-velocity surrounding rock, and, as a result, the recording site samples a different part of the radiation pattern than it otherwise would. The velocity change required to explain the observations corresponds to a P-wave time delay across the fault zone of the order of one-tenth of the values given by Healy and Peake (1975) and Marks and Bufe (1979) for some portions of the fault; thus it is quite reasonable to expect velocity changes of the required magnitude. The refraction of the rays near the surface and in the fault zone is calculated from Snell's law; the change in amplitude is calculated on the assumption that the energy flux along a tube of rays is constant.

To compute the synthetic seismograms, the dislocations at the source are replaced by the equivalent double couples, whose radiation field is calculated by the far-field formulas of Hirasawa (1970). The free-surface interaction is accounted for by applying complex reflection coefficients in the frequency domain. The solution thus includes the direct body waves but not surface waves. This should be an adequate approximation, at least for higher frequencies at sites near the source. Anelastic attenuation is accounted for by applying the Lomnitz causal Q operator described by Savage and O'Neill (1975), and another operator is applied to simulate the effect of the recording instrument.

EXAMPLE

To illustrate the method, we have chosen to model the Temblor strong-motion record from the Parkfield, California earthquake of 1966. This earthquake occurred on the San Andreas fault, a right-lateral strike-slip fault. The rupture propagated from the hypocenter toward the southeast for a distance that is the subject of some dispute. We adopt the interpretation of A. G. Lindh and D. M. Boore (unpublished manuscript), according to which the rupture propagated a distance of about 25 km from the hypocenter at a velocity of 2.5 km/sec. The Temblor station is 16 km southeast of the postulated end point of the rupture. Guided by the distribution of aftershocks (Eaton and others, 1970), we place the line source at a depth of 6 km and choose a fault width of 7 km. P and S velocities are assumed to be 6.0 and 3.5 km/sec, respectively, for the halfspace and 4.0 and 1.1, respectively, for the Franciscan rocks at the recording site. An S-wave Q of 100 is estimated from the spectrum of the observed strong-motion record and a P-wave Q of 220 is computed from the S-wave Q on the assumption of zero energy loss in compression. Independent estimates of Q would be desirable, but we have no other data for this area.

In fitting the observed strong-motion record we first adjust the velocities in the fault zone to fit the observed amplitude ratio between the horizontal components. A fit is obtained by reducing the velocities in the fault zone by 12 percent from the halfspace values. The coherence length ℓ_c is then varied to obtain the correct frequency content, and the standard deviation of the dislocation amplitude σ_D is varied to give the correct integral square amplitude. The results, using conditions (1) and

(2), are 190 cm for σ_D and $\bar{D}$, 0.73 km for ℓ_c, and 0.29 sec for τ.

In Figures 3, 4, and 5 synthetic accelerograms for three members of the ensemble (above) are compared with the observed record (below) for each of the three components. A similar comparison is shown in Figure 6 for the velocity on the transverse component and in Figure 7 for the Fourier spectrum of acceleration on the transverse component. Figure 8 shows the five-percent-damped, pseudovelocity response spectra for the transverse component. The plus signs represent the synthetic accelerograms and the line represents the observed record.

DISCUSSION

Figures 3 through 8 indicate that the synthetic seismograms have an amplitude envelope and a frequency content quite similar to the observed record. The synthetic seismograms lack the low-amplitude coda of surface waves and scattered body waves that is present on the observed record, but this discrepancy is probably of limited engineering significance, at least for high-frequency structures at short distances from the source.

The value of 190 cm for the mean dislocation, which results from our requirement that the mean be equal to the standard deviation, is rather high. The corresponding seismic moment of 1.1×10^{26} dyne-cm is more than twice as high as the value of 4.4×10^{25} obtained by Trifunac and Udwadia (1974) from an analysis of doubly integrated strong-motion records. The latter value in turn is about three times as high as that obtained by Tsai and Aki (1969) from long-period teleseismic surface waves. We do not believe, however, that these discrepancies indicate any serious defect in the method. For one thing, our requirement that the mean and the standard deviation be equal is to some degree arbitrary. For another, the record we are fitting is close to the southeast end of the fault and is significantly affected only by the dislocation near that end. Trifunac and Udwadia (1974) obtained a dislocation of 140 cm at the southeast end for a fault width of 6 km, which would correspond to a value of 120 cm for our fault width of 7 km, a value not too different from the one we obtained. The discrepancy with the teleseismic moment (Tsai and Aki, 1969) may in part be due to the fact that the teleseismic data is affected by the whole fault, whereas our site is significantly affected only by the southeast end.

We are encouraged by the comparisons of Figures 3 through 8 that this method will prove useful in generating time histories for dynamic analysis and in estimating ground motion parameters.

REFERENCES

Aki, K. (1967). Scaling law of seismic spectrum, J. Geophys. Res., v. 72, p. 1217-1231.

Butler, R., Kanamori, H., and Geller, R. (1975). Long-period ground motion in Los Angeles from a great earthquake on the San Andreas fault (abs.), Trans. Am. Geophys. Union, v. 56, p. 1024.

Bycroft, G. N. (1960). White noise representation of earthquake, Eng. Mech. Div., Am. Soc. Civil Engineers, v. 86, p. 1-16.

Eaton, J. P., O'Neill, M. E., and Murdock, J. N. (1970). Aftershocks of the 1966 Parkfield-Cholame, California, earthquake: a detailed study, Bull. Seism. Soc. Am., v. 60, p. 1151-1197.

Hanks, T. C. (1979). b values and $\omega^{-\gamma}$ seismic source models: implications for tectonic stress variations along active crustal fault zones and the estimation of high-frequency strong ground motion, J. Geophys. Res., v. 84, p. 2235-2242.

Haskell, N. A. (1966). Total energy and energy spectral density of elastic wave radiation from propagating faults. Part II. A statistical source model, Bull. Seism. Soc. Am., v. 56, p. 125-140.

Healy, J. H., and Peake, L. G. (1975). Seismic velocity structure along a section of the San Andreas fault near Bear Valley, California, Bull. Seism. Soc. Am., v. 65, p. 1177-1197.

Hirasawa, T. (1970). Focal mechanism determination from S wave observations of different quality, J. Phys. Earth, v. 18, p. 285-294.

Housner, G. W. (1955). Properties of strong ground motion earthquakes, Bull. Seism. Soc. Am., v. 45, p. 197-218.

Housner, G. W., and Jennings, P. C. (1964). Generation of artificial earthquakes, Eng. Mech. Div., Am. Soc. Civil Engineers, v. 90, p. 113-150.

Jurkevics, A., and Ulrych, T. J. (1978). Representing and simulating strong ground motion, Bull. Seism. Soc. Am., v. 68, p. 781-801.

Marks, S. M., and Bufe, C. G. (1979). Fault-crossing P delays, epicentral biasing, and fault behavior in central California (abs.), Tectonophys., v. 52, p. 600.

Mayer-Rosa, D. (1973). Travel-time anomalies and distribution of earthquakes along the Calaveras fault zone, California, Bull. Seism Soc. Am., v. 63, p. 713-729.

Rascon, O. A., and Cornell, C. A. (1969). A physically based model to simulate strong earthquake records on firm ground, Proceedings of the Fourth World Conference on Earthquake Engineering, Santiago, Chile, v. 1, p. A1-84 to A1-96.

Savage, J. C., and O'Neill, M. E. (1975). The relation between the Lomnitz and Futterman theories of internal friction, J. Geophys. Res., v. 80, p. 249-251.

Trifunac, M. D., and Udwadia, F. E. (1974). Parkfield, California, earthquake of June 27, 1966: a three-dimensional moving dislocation, Bull. Seism. Soc. Am., v. 64, p. 511-533.

Tsai, Y. B. and Aki, K. (1969). Simultaneous determination of the seismic moment and attenuation of seismic surface waves, Bull. Seism. Soc. Am., v. 59, p. 275-287.

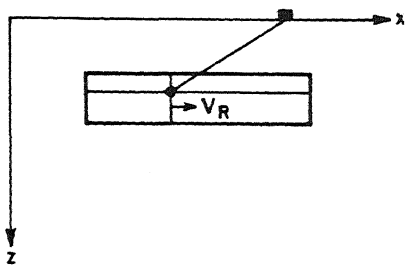

Figure 1. Diagrammatic vertical section showing the source model. V_R is the rupture velocity.

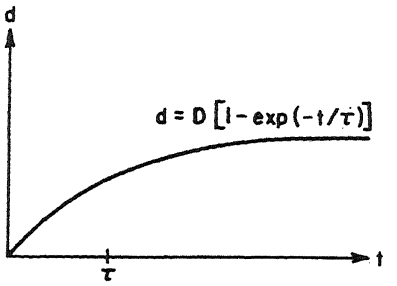

Figure 2. Dislocation d as a function of time t.

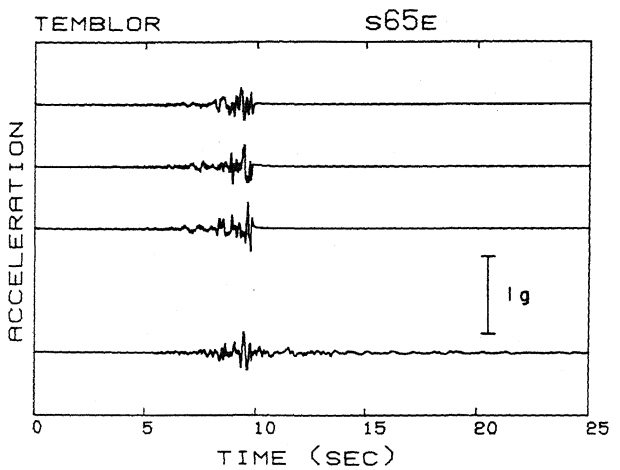

Figure 3. The radial component of acceleration. Three synthetic accelerograms above and real record below.

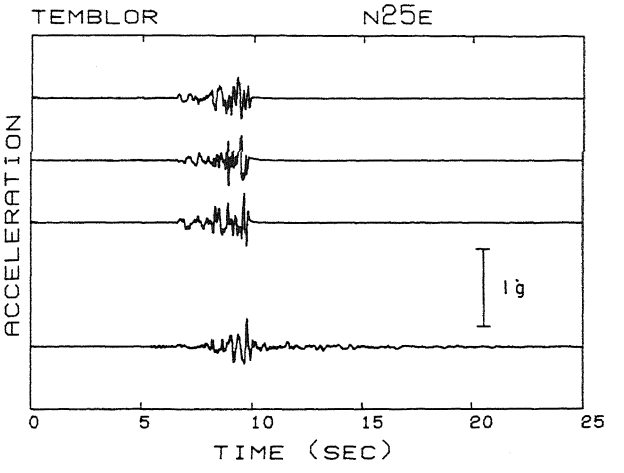

Figure 4. The transverse component of acceleration. Arrangement as in Figure 3.

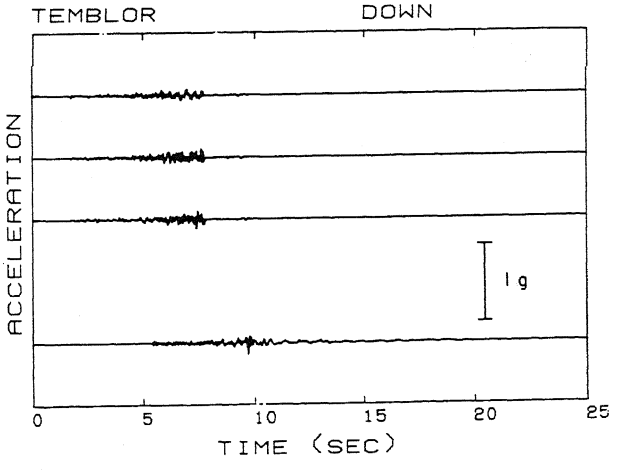

Figure 5. Vertical acceleration. Arrangement as in Figure 3.

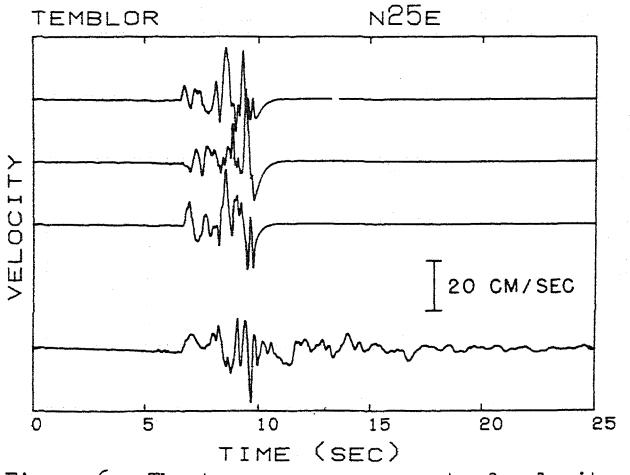

Figure 6. The transverse component of velocity. Arrangement as in Figure 3.

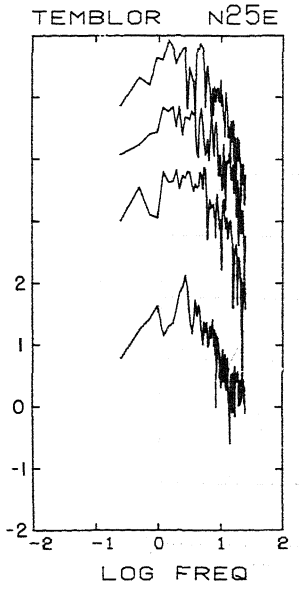

Figure 7. Common logarithm of acceleration spectra (cm/sec) for the transverse component. Spectra for the three synthetic accelerograms (above) are shifted vertically for ease of comparison; the spectrum of the real record is plotted to the scale indicated.

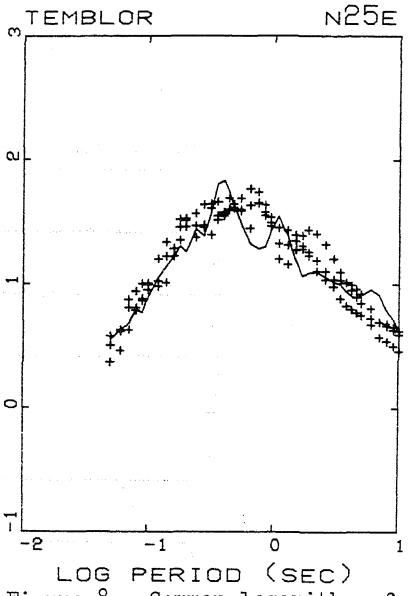

Figure 8. Common logarithm of pseudovelocity response spectra (cm/sec) for the transverse component five percent damping. Plus signs represent the synthetic accelerograms; the line represents the real record.